A highly efficient $Cu/ZnO/Al_2O_3$ catalyst via gel-coprecipitation of oxalate precursors for low-temperature steam reforming of methanol

Xin-Rong Zhang, Lu-Cum Wang, Cheng-Zhang Yao, Yong Cao* Wei-Lin Dai, He-Yong He, and Kang-Nian Fan

Department of Chemistry and Shanghai Key Laboratory of Molecular Catalysis and Innovative Materials, Fudan University, Shanghai, 200433 P. R. China

The impact of preparation methods on the structure and catalytic behavior of $Cu/ZnO/Al_2O_3$ catalysts for H_2 production from steam reforming of methanol (SRM) has been reported. The results show that the nanostructured $Cu/ZnO/Al_2O_3$ catalyst obtained by a novel gel-coprecipitation of oxalate precursors has a high specific surface area and high component dispersion, exhibiting much higher activity in the SRM reaction as compared to the catalysts prepared by conventional coprecipitation techniques. It is suggested that the superior catalytic performance of the oxalate gel-coprecipitation-derived $Cu/ZnO/Al_2O_3$ catalyst could be attributed to the generation of "catalytically active" copper material with a much higher metallic copper specific surface as well as a stronger Cu–Zn interaction due to an easier incorporation of zinc species into $CuC_2O_4 \cdot x\, H_2O$ precursors as a consequence of isomorphous substitution between copper and zinc in the oxalate gel-precursors.

KEY WORDS: oxalate gel-coprecipitation; $Cu/ZnO/Al_2O_3$ catalyst; steam reforming of methanol; hydrogen production.

1. Introduction

Steam reforming of methanol (SRM) provides an attractive and viable technology for use in catalytic generation of hydrogen to produce clean electrical energy from fuel cells [1–5]. Copper-containing catalysts, especially CuO/ZnO and $CuO/ZnO/Al_2O_3$ mixed oxides, have been the most frequently studied catalysts in this process, due to their high selectivity and activity [6–10]. Generally, these catalysts require temperatures as high as 280 °C for efficient operation. From a practical viewpoint, it is desirable to operate the reformer at lower reaction temperatures due to the temperature mismatch between the reactor and the fuel cell [5]. Moreover, the high reaction temperature tends to result in the production of CO—a poison to the promising proton-exchange membrane (PEM) fuel cells [3–5]. Therefore, new improved catalyst systems that can allow the effective production of hydrogen free from carbon monoxide at lower reaction temperatures are highly desired.

Regarding the synthesis of Cu/Zn-based mixed oxide catalysts, the coprecipitation of a hydroxycarbonate (HC) precursor followed by calcination has shown to be practical for commercial production of $Cu/ZnO/Al_2O_3$ catalysts for methanol synthesis or the water–gas shift reaction [8–10]. However, this ill-defined process often has disadvantages, such as tedious multistep processing and the need for delicate pH and temperature control. Additionally, the final material obtained from this pro-cess is always suffered from the contamination of alkaline metals [10]. To circumvent above problems, it is important to develop more suitable method for preparation of the $Cu/ZnO/Al_2O_3$ catalyst system with tailored properties, Recently, we have reported that copper and zinc could be effectively dispersed by an easily controlled approach based on the gel-coprecipitation oxalate precursor from alcoholic solution, resulting in the formation of nanostructured $Cu/ZnO/Al_2O_3$ catalyst featured by a much higher copper surface area with improved copper dispersion [11–13]. The $Cu/ZnO/Al_2O_3$ catalyst prepared by the oxalate gel-coprecipitation method is found to be highly efficient for methanol synthesis from CO_2 hydrogenation [11–13]. On considering that the SRM reaction ($CH_3OH + H_2O \rightarrow 3H_2 + CO_2$) could be viewed as a chemical reverse with respect to the methanol synthesis from CO_2 hydrogenation, it is conceivable that the oxalate gel-coprecipitation method may also provide attractive alternative for fabricating new efficient catalyst system for the SRM.

In the present work, the preparation of the new nanostructured $Cu/ZnO/Al_2O_3$ catalyst by gel-coprecipitation of oxalate precursor as well as its superior performance in the SRM reaction is reported, The influence of the preparation method on the catalytic behavior of the $Cu/ZnO/Al_2O_3$ catalysts is also presented. It is demonstrated that the oxalate gel-coprecipitation method, previously established to be an effective technique for the preparation of the nanostructured $Cu/ZnO/Al_2O_3$ catalyst highly efficient for methanol synthesis from CO_2 hydrogenation by our

*To whom correspondence should be addressed.
E-mail: yongcao@fudan.edu.cn

group [11–13], has shown to be particularly useful in generating the highly active Cu/ZnO/Al$_2$O$_3$ catalyst for the low temperature SRM.

2. Experimental

2.1. Preparation of catalyst

Three Cu/ZnO/Al$_2$O$_3$ catalysts, all with a molar ratio of copper, zinc and aluminum 45:45:10 were prepared by different methods. A typical procedure to prepare the gel-coprecipitated oxalate precursor CZA01 is as follows: an alcoholic solution of 20% excess of oxalic acid is injected rapidly into a mixed alcoholic solution (each 0.1 M) of copper nitrate, zinc nitrate, aluminum nitrate at room temperature at vigorous stirring. The gel-like precipitates are formed and separated by centrifuge, then dried at 110 °C overnight, which show significant volume shrinkage during the drying process. The procedure to prepare precursor CZA02 is similar to the procedure for preparing the precursor CZA01. The only difference is that an aqueous solution is used as a replacement of the alcoholic solution as described above. The precursor CZA03 is prepared by the conventional carbonate co-precipitation method. Briefly, a mixed aqueous solution of copper nitrate, zinc nitrate, and aluminum nitrate (each 0.1 M) and a solution of sodium carbonate (0.1 M) were added slowly and simultaneously into 150 mL of deionized water at 80 °C with vigorous stirring. The pH was kept constant at 6.5–7.0. The precipitates were aged at 50 °C for 30 min under vigorous stirring, then filtered and thoroughly washed with warm deionized water. The precipitates were dried overnight in air at 110 °C.

All precipitates were calcined in a muffle oven at 150 °C for 1 h, 200 °C for 1 h, 250 °C for 1 h, 300 °C for 1 h and 360 °C for 4 h.

2.2. Catalyst characterization

The textural parameters have been measured using the BET method by N$_2$ adsorption and desorption at 77 K in a Micromeritics TriStar system. Transmission Electron Microscopy (TEM) was recorded digitally with a Gatan slow-scan charge-coupled device (CCD) camera on a JEOL 2011 electron microscope operating at 200 kV. The samples were prepared by dispersing the powder products as a slurry in acetone, which was then deposited and dried on a holey carbon film on a Cu grid: The X-ray powder diffraction (XRD) of the samples was carried out on a Germany Bruker D8Advanee X-ray diffractometer using nickel filtered Cu Kα radiation at 40 kV and 20 mA. *In situ* XRD experiments performed are as follows: reduction of the calcined Cu/ZnO/Al$_2$O$_3$ precursors in 5 vol% H$_2$ in argon in a temperature range from room temperature to 250 °C at a heating ramp of 1 °C min^{-1} was carried out in a XRK-900 high

temperature cell. *In situ* XRD patterns were recorded at 230 °C under simulated methanol steam reforming conditions (c(MeOH) $\sim$ 5 vol%, c(H$_2$O) $\sim$ 5.5 vol% in 100 mL min^{-1} Ar) (20–80° 2θ, step width 0.02° 2θ, counting time: 1s/dp (dp = data point)). XRD patterns of the various Cu/ZnO/Al$_2$O$_3$ catalysts under reaction conditions were analyzed by the Pawley method ("full pattern refinement"). The crystallite size corresponding to the broadening of each *hkl* line was determined from the Lorentzian part of the individual profile functions. The specific copper surface areas as calculated from the crystallite size assuming a spherical particle, are in good agreement with the results of the N$_2$O titration. The specific area of metallic copper was calculated from the total amount of N$_2$O consumption with 1.46×10^{19} copper atoms per [14–16]. The accuracy of the metallic copper surface area measurement was higher than 95%. TPR profiles were measured under the following conditions: heating rate 5 °C min^{-1}, flow-rate 40 mL min^{-1} 5%H$_2$/Ar.

2.3. Activity tests

Catalytic experiments were performed at atmospheric pressure in a continuous flow fixed-bed microreactor consisting of a stainless-steel tube with an internal diameter of 10 mm and a coaxially centered thermocouple with its tip located in the middle of the bed. Prior to each experiment, the catalyst (40–60 mesh size, 0.5 g) packed in the stainless-steel reactor is reduced at 250 °C for 6 h in flowing premixed H$_2$/Ar(5/95) flow of 80 mL min^{-1}. After reduction, the premixed water and methanol was then pumped to the vaporizer maintained at about 250 °C. The vaporized feed entered the reactor with a stream of Ar gas, which had a speed of 30 mL min^{-1}, and then began the steam reforming reaction at the designated reaction temperature. The reaction was carried out under the following conditions: pressure: 0.1 MPa; reaction temperature: 180–250 °C; liquid feed (H$_2$O/methanol = 1.1 molar ratio): 2.35–9 mL h^{-1}; WHSV = 4–15.5 h^{-1}. All experimental data were obtained under steady-state conditions that were usually maintained for several hours before changing the reaction conditions to obtain another set of data.

The reaction products were analyzed on-line by a gas chromatograph. The GC was equipped with a thermal conductivity detector and two packed columns in series were used to separate reaction products (one for separation of polar components, i.e., CO$_2$, water, methanol, formaldehyde, methyl formate, and DME, and a molecular sieve for separation of H$_2$, O$_2$, N$_2$, and CO). Blank run conducted with an empty reactor in a temperature range of 180–250 °C did not show any detectable methanol conversion. In the following text, the product gas composition refers to the composition of the gas stream leaving the reactor.

3. Results and discussion

3.1. Characterization of the catalysts

The XRD patterns of the catalyst precursors prepared by conventional oxalate coprecipitation and the present gel-oxalate coprecipitation method are shown in figure 1. The precursor of the conventional oxalate method exhibited three sharp peaks at 18.7°, 22.9° and 23.7°, which were identified as diffraction lines of αZn-$C_2O_4 \cdot 2H_2O$, $CuC_2O_4 \cdot xH_2O$, and β-$ZnC_2O_4 \cdot 2H_2O$, respectively, However, no diffraction bands corresponding to zinc-containing phases can be found in XRD patterns of the precursor obtained from the novel method. This indicates that zinc phase existed in very fine crystallites and most zinc was incorporated into the $CuC_2O_4 \cdot xH_2O$ structure, because little water was present under these conditions and isomorphous substitution between copper and zinc was allowed [12]. Moreover, the diffraction peaks of CZA01 are much broader than those of the catalyst prepared by the conventional oxalate method, which indicates that the average particle size of the precipitates prepared by the novel method are much smaller than those of the conventional method.

The XRD patterns of the calcined catalyst precursors obtained by the conventional aqueous oxalate coprecipitation, the oxalate gel-coprecipitation as well as the conventional carbonate co-precipitation method are presented in figure 2. It is shown that broad diffraction lines corresponding to CuO and ZnO are observed, indicating the chemically homogeneous nature of the calcined samples. It is noticeable that no peaks of Al_2O_3 could be observed, which suggests that the particles of Al_2O_3 are either amorphous in phase or very fine and highly dispersed in the catalyst [14–16]. As shown in Figure 2, the diffraction peaks of CuO and ZnO for CZA01 catalyst are much broader and lower as compared to those of catalyst prepared by the conventional oxalate method and the conventional carbonate co-precipitation method. This indicates that the crystallite size of ZnO and CuO in catalyst precursor of CZA01 are much smaller than that in precursor CZA02 and CZA03.

The results of the physicochemical properties of the calcined catalysts prepared by the oxalate gel-coprecipitation method are presented in table 1. For comparison, the physicochemical properties of the catalysts obtained by the conventional methods using oxalic acid as well as sodium carbonate as precipitation agents are also included. One can see that both the BET specific surface area and the copper metal surface area of the catalyst prepared by the present oxalate gel-coprecipitation method are significantly higher than that prepared by the conventional methods. It is noticeable that sample CZA02 exhibits the lowest BET surface area and smallest pore volume. Copper surface areas measured by nitrous oxide titration are also listed in table 1. By using a quasi-sphere model, the average copper metal crystallite sizes were calculated from the copper surface areas. The data of the metallic copper surface area in table 1 demonstrate clearly that the copper dispersion in CZA01 catalyst is much higher than that of catalysts prepared by the conventional methods. It is therefore expected that the catalyst derived by oxalate gel-coprecipitation can provide catalytically active centers consisting of copper nanoparticles with much smaller crystallite size for hydrogen production from SRM reaction.
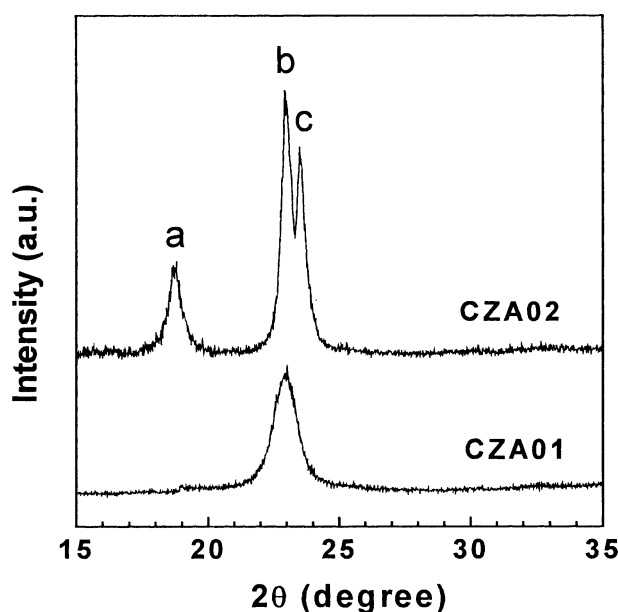

Figure 1. XRD patterns of the precipitates prepared by conventional oxalate co-precipitation and oxalate gel-coprecipitation methods. (a) α-$ZnC_2O_4 \cdot 2H_2O$; (b) $CuC_2O_4 \cdot xH_2O$; and (c) β-$ZnC_2O_4 \cdot 2H_2O$.
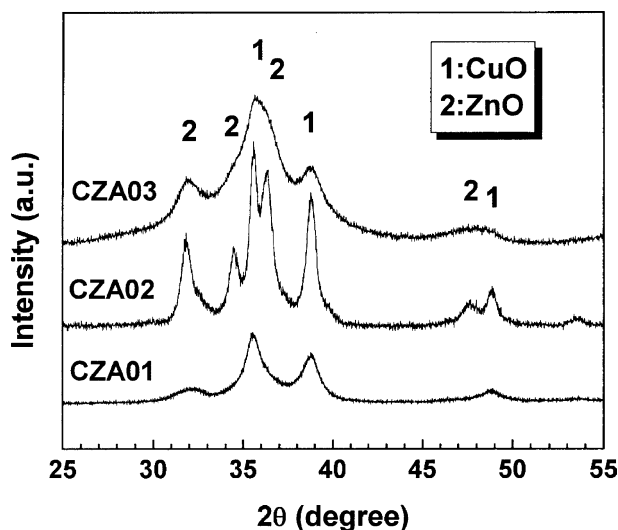
Figure 2. XRD patterns of the calcined catalysts prepared by various methods.

The TEM images of $Cu/ZnO/Al_2O_3$ calcined catalysts prepared by the oxalate gel-coprecipitation method and the conventional oxalate co-precipitation method are shown in figure 3. The morphology of the two calcined catalysts clearly demonstrates that the catalyst obtained by the conventional aqueous oxalate coprecipitation method consists of much larger particles of similar shape, which often appeared in much larger agglomerates than the catalyst prepared by the gel oxalate-coprecipitation method. It is seen that the CZA01 catalyst consisted of agglomeration of interconnected particle with sizes of ca. 10–15 nm. This is in good agreement with the above results from XRD and metallic copper surface area measurement. As a comparison, the intrinsic particles for CZA02 sample were aggregated into agglomerates with larger than 20 nm in size, further confirming the structural information derived form the XRD data.

To gain a further insight into the microstructural properties of the active $Cu/ZnO/Al_2O_3$ catalyst under working conditions, the *in situ* XRD investigations performed during SRM reaction were shown in figure 4. A detailed analysis of the Cu 111 diffraction line reveals a much larger copper particle size for CZA02 (26.3 nm) as compared to CZA01(10.2 nm) and CZA03 (17.3 nm). In addition, the diffraction lines of Cu and ZnO,

especially ZnO, are very weak and broadened, suggesting that zinc components were highly dispersed and exhibited "X-ray amorphous" features due to the formation of amorphous and/or microcrystallites during reduction [12]. This again unambiguously confirms that the present oxalate gel-coprecipitation method is particularly useful for preparing nanostructured $Cu/ZnO/Al_2O_3$ catalysts with high component dispersion.

In order to investigate the reducibility of the copper species in the $Cu/ZnO/Al_2O_3$ catalysts prepared by various methods, TPR measurements were carried out. The TPR profiles of the $Cu/ZnO/Al_2O_3$ catalysts prepared by oxalate gel-coprecipitation and conventional coprecipitation methods are reported in figure 5. For comparison, the TPR profile of the catalyst prepared by the conventional carbonate coprecipitation method is also presented. The TPR profiles of all three catalysts are featured by the presence of a single reduction peak. It is seen that the reduction peak of CZA01 is located at 226 °C, and those of CZA02 and CZA03 at 216 °C and 222 °C, respectively. It is noticed that a higher reduction temperature is needed to reduce the CuO in the oxalate gel-coprecipitation derived catalyst than the catalysts obtained by conventional coprecipitation methods, which however has a higher copper dispersion than the other two samples. Note that a better dispersion is always associated with an easier reduction of the copper species as a consequence of a stronger Cu/Zn interaction in the Cu/ZnO catalyst systems [10, 17]. Nevertheless, a similar shift of the reduction maximum toward higher temperature has been previously observed by Robinson and Moi [18] in a TPR study of the interaction of CuO and ZnO. They have attributed this phenomenon to the presence of a specific type of strong interaction between CuO and the ZnO lattice.

3.2. Catalytic activity

The SRM experiments were conducted with steam in excess of stoichiometry ($H_2O/CH_3OH = 1.1$ molar ratio), ensuring complete methanol conversion and suppressing CO formation by the reverse water–gas shift reaction ($CO_2 + H_2 \rightarrow H_2O + CO$). Catalytic activity was evaluated in terms of methanol conversion (mol.%) and hydrogen production rate (R_{H2}). Methanol steam reforming reaction on $Cu/ZnO/Al_2O_3$ catalysts in a wide temperature range showed that it was even very active at

Table 1

Physicochemical properties of the Cu/ZnO/Al₂O₃ catalysts prepared via various methods

Catalyst	S_{BET} ($m^2\ g^{-1}$)	Pore volume ($mL\ g^{-1}$)	Pore size (nm)	S_{cu}[a] ($m^2\ g^{-1}$)	d_{cu}[b] (nm)
CZA01	70.8	0.26	14.7	26.7	10.2
CZA02	46.8	0.20	16.3	11.5	26.3
CZA03	48.7	0.14	10.1	17.2	17.3

[a] Cu surface area measured by N_2O method after 5% H_2/Ar reduction.
[b] d_{Cu} calculated from *in situ* XRD data based on Sherrer equation.
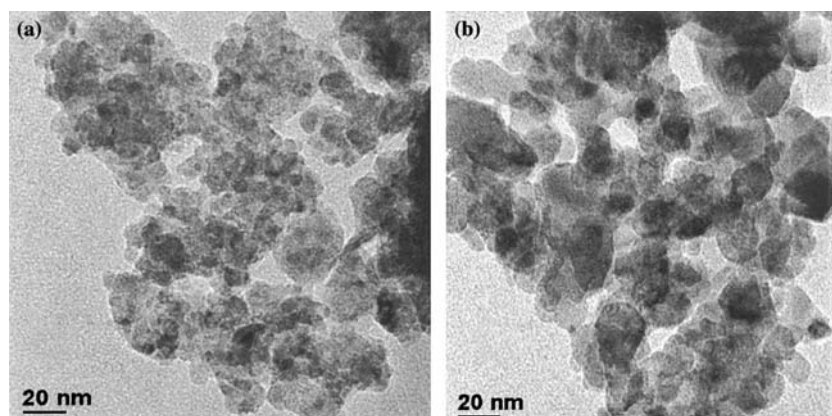
Figure 3. TEM images of calcined catalysts derived from (a) CZA01 and (b) CZA02.

a temperature as low as 180 °C. Analysis of the effluent gas indicated that H_2 and CO_2 were major components accompanied with a minor amount of CO. The amount of CO by-product produced was always below the detectable limit for the TCD under these conditions at lower reaction temperature, indicating that CO_2 selectivity was always greater than 99.0%, Other researchers have reported trends in CO selectivity when methanol conversion was close to 100% for various Cu-based catalysts [19]. The concentration of methane were always below 10 ppm, and therefore undetectable. Other products such as formaldehyde, formic acid, methyl formate and dimethyl ether formed during reactions of methanol on Cu-based catalysts could not be detected under the reaction conditions, the concentration for any of these by-products was never more than 500 ppm [20–22].

The catalytic performance of Cu/ZnO/Al₂O₃ catalysts for SRM is shown in figure 6. It can be clearly seen that the preparation methods have a significant influence on the performance of the catalyst for hydrogen production from SRM. Among them, CZA01 exhibit the highest methanol conversion and H_2 production rate throughout the temperature range studied. It is remarkable that a total conversion of methanol could be achieved over the CZA01 sample at a relatively low temperature of 250 °C. It is also highly interesting to make a comparison of the selectivity toward CO formation for all three catalysts. As shown in figure 6. The CO selectivity is observed to be less than 1.0% over CZA01 in the temperature range of 180–250 °C, however, CZA02 and CZA03 show relatively higher selectivity for CO formation. These results imply that the catalyst prepared by the oxalate gel-coprecipitation method can effectively retard the formation of CO and exhibit high selectivity for CO_2 during methanol steam reforming.

The effect of reaction temperature on the catalytic performance of Cu/ZnO/Al₂O₃ catalysts is also illustrated
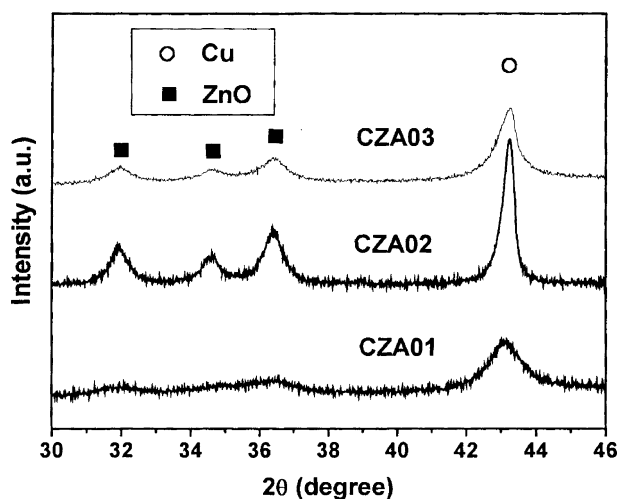

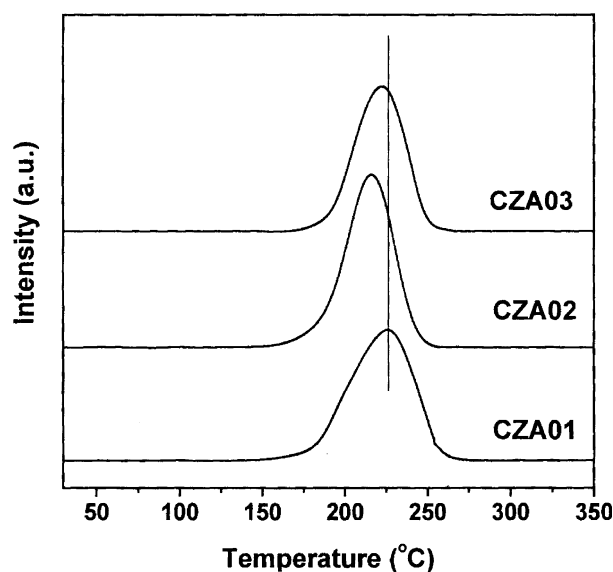Figure 4. *In-situ* XRD patterns of the calcined catalysts prepared by various methods during SRM.

Figure 5. TPR profiles of Cu/ZnO/Al₂O₃ catalysts prepared via various methods.

in figure 6. It can be seen that methanol conversion and H_2 production rate increase with increasing reaction temperature, while methanol is converted almost completely into H_2 and CO_2 accompanied with trace amount of CO up to 250 °C over the CZA01 catalyst. At lower temperature reactions, especially at 180 °C, CZA01 exhibits much higher activity as compared with CZA02 and CZA03, methanol conversion is up to 63.9%. All $Cu/ZnO/Al_2O_3$ catalysts exhibit a high selectivity for H_2 production and relatively low selectivity for CO generation in the temperature range of 180–250 °C. On the

other hand, CO selectivity increases at high reaction temperature.

The catalytic activity of the $Cu/ZnO/Al_2O_3$ catalysts is also found to be strongly dependent on the space velocity (WHSV) of the liquid feeding. Figure 7 shows the effect of WHSV on the catalytic performance of the CZA01 catalyst. It can be seen that both methanol conversion and the selectivity to CO decrease rapidly with the increase of WHSV, whereas the selectivity to hydrogen is maintained at the same level around 99.9%. However, the hydrogen production rate is observed to increase rapidly with increasing methanol space velocity, with the highest hydrogen production rate being achieved at a high WHSV of about 15.5 h^{-1}.

3.3. Discussion

Previous investigations concerning the use of copper-based catalysts for methanol steam reforming have revealed that methanol conversion over Cu/Zn-based catalysts greatly depends on the status of copper, such as the dispersion, metal surface area and particle size [6–10, 23, 24]. Catalyst with high copper dispersion shows better performance in methanol steam reforming. The status of metal dispersion should be closely related to overall surface area. Unfortunately, the Cu/Zn-based
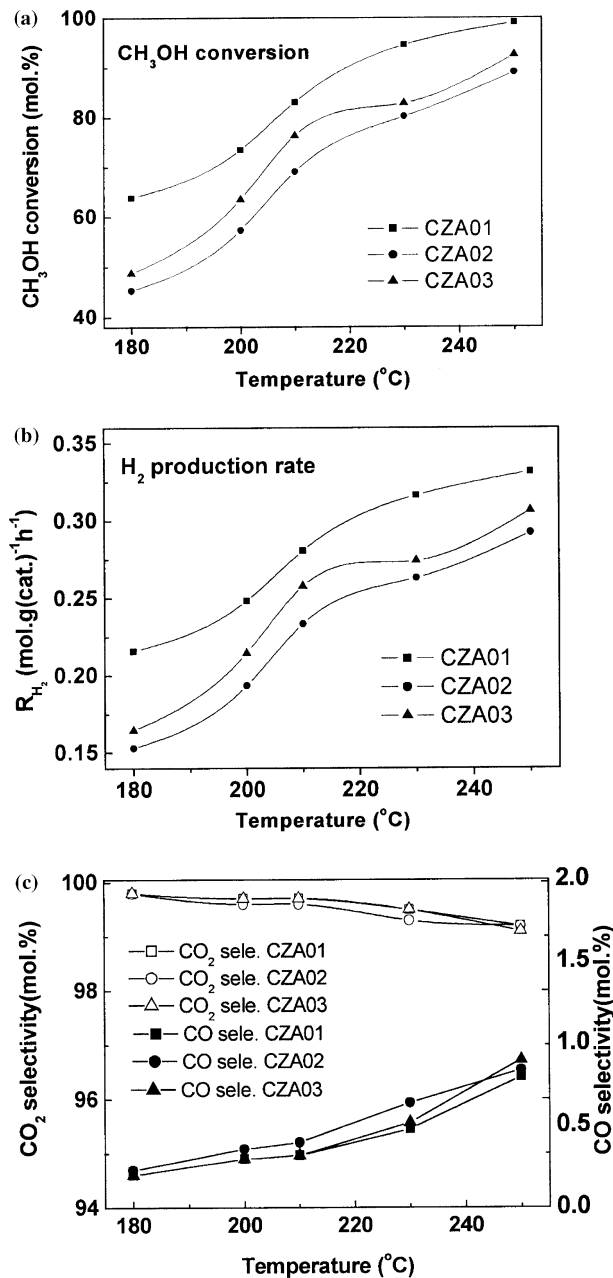

Figure 6. Effect of reaction temperature on catalytic activity over of $Cu/ZnO/Al_2O_3$ catalysts prepared via various methods. (reaction conditions: $H_2O/CH_3OH = 1.1$ molar ratio; WHSV, ~5.8 h^{-1}; pressure, ~0.1 MPa.)
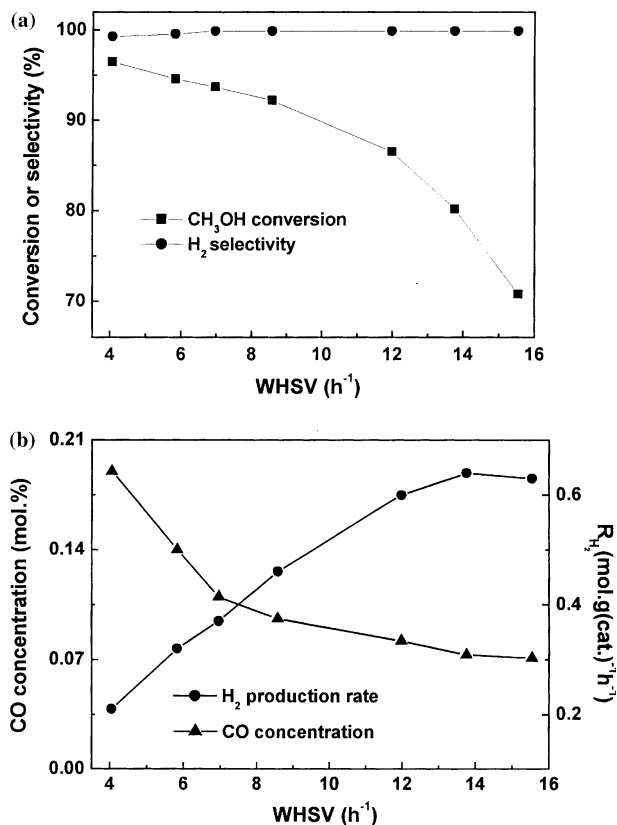

Figure 7. Effect of liquid feed space velocity (WHSV) on catalytic activity over the CZA01 catalyst. (reaction conditions: $H_2O/CH_3OH = 1.1$ molar ratio; $T = 230$ °C; pressure, ~0.1 MPa.)

catalysts generally appear to have low surface area by conventional preparation methods, In our case, the results show unambiguously that the present new process utilizing the oxalate gel-coprecipitation method can allow the generation of $Cu/ZnO/Al_2O_3$ catalyst with a much higher specific surface area and improved copper dispersion with respect to those of conventional catalysts. The $Cu/ZnO/Al_2O_3$ catalyst obtained by gel-coprecipitation of oxalate precursor has demonstrated a unique catalytic behavior in methanol steam reforming as compared to the catalysts prepared by other methods in terms of methanol conversion, H_2 yield and CO concentration. It is remarkable that a high methanol conversion of ca. 94.6% at a relatively low reaction temperature of 230 °C could be achieved over the oxalate gel-coprecipitation derived $Cu/ZnO/Al_2O_3$ catalyst.

Regarding the essential nature of metallic copper for catalytic production of H_2 from methanol steam reforming, some studies have experimentally demonstrated that for a given type of catalyst, the catalytic activity is proportional to the metallic copper surface area [25–27]. Apparently, the catalytic activity results (see figure 6) show that a high Cu surface area is a prerequisite for an active $Cu/ZnO/Al_2O_3$ catalyst. As shown in table 1, the high catalytic performance of the catalyst prepared by the oxalate gel co-precipitation method could be related to higher metal copper surface area as described above. Furthermore, the improved synergy effect between active Cu material and Zn species as a consequence of a higher component dispersion and smaller crystallite size of the active component is also thought to be essential for the enhanced catalytic performance in the SRM reaction. Similar results were also reported very recently in the SRM over Cu/Zn-based catalysts [28, 29]. Our previous studies [12, 30] also have suggested that, although high metallic copper surface area is very important and necessary for a highly active $Cu/ZnO/Al_2O_3$ methanol synthesis catalyst, the interaction or synergy between copper species and zinc oxide could also have an important impact on catalytic activity of the catalyst.

On the other hand, it is also interesting to note that the most active catalyst CZA01 prepared by the present oxalate-gel coprecipitation method had the highest TPR peak and was even active for the SRM reaction at much lower temperatures. Previous investigations concerning the reducibility of copper-based catalysts for methanol synthesis have revealed that a better reducibility is always associated with a higher activity of the catalyst [17]. However, according to a recent investigation by Gunter *et al.* [10], this does not necessarily mean that the reducibility of copper species is the decisive parameter in determining the catalytic performance of the present $Cu/ZnO/Al_2O_3$ samples. Actually, it would be highly interesting to point out that a less sintering is expected for the reductive activation of catalyst CZA01 thus leading to the generation of much smaller copper

particles in the active catalyst. This could be the main reason why the less reducible CZA01 shows an improved performance of for SRM reaction.

Based on the present investigation, it is clear that the superior catalytic performance of the oxalate gel-coprecipitation derived $Cu/ZnO/Al_2O_3$ catalyst can be attributed to the particularly high copper surface area, the small crystallite size of copper particles and a stronger interaction between the copper species and the ZnO lattice [12, 31]. Obviously, the oxalate gel-coprecipitation method, previously established to be an effective technique for the preparation of the ultrafine $Cu/ZnO/Al_2O_3$ catalyst highly efficient for methanol synthesis from CO_2 hydrogenation by our group [11–13], has been experimentally demonstrated to be particularly useful in generating the highly active $Cu/ZnO/Al_2O_3$ catalyst for the low temperature SRM.

4. Conclusions

In summary, the preparation methods have a significant influence on the structure of the catalyst and catalytic activity for hydrogen production from SRM. It is shown that the oxalate gel-coprecipitation approach involving the gel-coprecipitation of oxalate precursors can allow the fabrication of new improved $Cu/ZnO/Al_2O_3$ catalyst with high surface area and high component dispersion, which exhibits a much higher catalytic activity for low temperature SRM than the catalysts prepared by conventional coprecipitation techniques. Combined XRD, TEM and TPR results demonstrated that the superior catalytic performance of the oxalate gel-coprecipitation derived $Cu/ZnO/Al_2O_3$ catalysts could be attributed to the generation of highly dispersed copper and zinc components as well as the creation of "catalytically active" copper species with a much higher metallic copper specific surface and a stronger Cu–Zn interaction due to an easier incorporation of zinc species into $CuC_2O_4 \cdot xH_2O$ precursors as a consequence of isomorphous substitution between copper and zinc in the oxalate gel-precursors.

References

[1] W. Wies and B. Emonts, J. Power Sources 84 (1999) 187.
[2] J.C. Amphlett and R.F. Mann, J. Power Sources 71 (1998) 179.
[3] J. Agrell, M. Boutonnet, I. Melián-Cabrera and J.L.G. Fierro, Appl.Catal. A 253 (2003) 201.

[4] J. Agrell, M. Boutonnet and J.L.G Fierro, Appl. Catal. A 253 (2003) 213.

[5] S. Velu, K. Suzuki, M. Okazaki, M.P. Kapoor, T. Osaki and F. Ohashi, J. Catal. 194 (2000) 373.

[6] J.P. Shen and C.S. Song, Catal. Today 77 (2002) 89.

[7] P.J. Wild and M.J.F.M. Verhaak, Catal. Today 60 (2000) 3.

[8] S. Murcia-Mascaros, R.M. Navarro, L. Gomez-Sainero, U. Costantino, M. Occhetti and J.L.G. Fierro, J. Catal. 198 (2001) 338.

[9] R.M. Navarro, M.A. Pena and J.L.G. Fierro, J. Catal. 212 (2002) 112.

[10] M.M. Gunter, T. Ressler, R.E. Jentoft and B. Bwms, J. Catal. 203 (2001) 133.

[11] J.F. Deng, Q. Sun, Y.L. Zhang, H.Y. Chen and D. Wu, Appl. Catal. A 139 (1996) 75.

[12] Q. Sun, Y.L. Zhang, H.Y. Chen and J.F. Deng, J. Catal. 167 (1997) 92.

[13] Y.L. Zhang, Q. Sun, J.F. Deng, D. Wu and S.Y. Hen, Appl. Catal. A 158 (1997) 105.

[14] G.C. Chinchen, C.M. Hay, H.D. Vandervell and K.C. Waugh, J. Catal. 103 (1987) 79.

[15] J.B. Friedrich, M.S. Wainwaight and D.J. Young, J. Catal. 80 (1983) 1.

[16] J.W. Evans, M.S. Wainwright, A.J. Bridgewater and D.J. Young, Appl. Catal. A 7 (1983) 75.

[17] G. Fierro, M.Lo. Jacono, M. Inversi, P. Pporta, F. Cioci and R. Lavecchia, Appl. Catal. 76 (1991) 117.

[18] W.R.A.M. Robinson and J.C. Moi, Appl. Catal. 76 (1991) 117.

[19] J. Agrell, H. Birgersson, M. Boutonnet, I. Melian-Cabrera, R.M. Navarro and J.L.G. Fierro, J. Catal. 219 (2003) 389.

[20] P.H. Matter, D.J. Braden and U.S. Ozkan, J. Catal. 223 (2004) 340.

[21] S. Velu, K. Suzuki and T. Osaki, Catal. Lett. 62 (1999) 159.

[22] I.E. Wachs and R.J. Madix, J. Catal. 53 (1978) 208.

[23] R.A. Koeppel, A. Baiker and A. Wokaun, Appl. Catal. A 184 (1992) 77.

[24] Y. Nitta, T. Fujimatsu, Y. Okamoto and T. Imanaka, Catal. Lett. 17 (1993) 157.

[25] G.C. Chinchen, K.C. Waugh and D.A. Whan, Appl. Catal. A 25 (1986) 101.

[26] G.C. Chinchen, P.G. Parker and G.D. Short, Prepr. Am. Chem. Soc. Div. Fuel Chem 29 (1984) 178.

[27] B. Denise, P.R.A. Sneedn, B. Beguin and O. Cherifi, Appl. Catal. A 30 (1987) 353.

[28] J.P. Breen and J.R.H. Ross, Catal. Today 51 (1999) 521.

[29] J.P. Breen, F.C. Meunier and J.R.H. Ross, Chem. Commun. 2247 (1999) –.

[30] Y. Ma, Q. Sun, D. Wu, W.H. Fan and J.F. Deng, Appl. Catal. A 177 (1999) 177.

[31] A.L. Boyce, P.A. Sermon, M.S.W. Vong and M.A. Yates, React. Kinet. Catal. Lett. 44 (1991) 309.